Flow of a Non-Newtonian Nanofluid Between Coaxial Cylinders with Variable Viscosity

Muhammad Yousaf Malik, Azad Hussain, and Sohail Nadeem

Department of Mathematics, Quaid-i-Azam University 45320, Islamabad 44000 Pakistan

Reprint requests to M. Y. M.; E-mail: drmymalik@hotmail.com

Z. Naturforsch. **67a,** 255 – 261 (2012) / DOI: 10.5560/ZNA.2012-0018
Received July 7, 2011 / revised December 27, 2011

In the present paper, we have focused our attention to highlight the study of a non-Newtonian nanofluid between coaxial cylinders with variable viscosity. The governing equations of the non-Newtonian fluid with variable viscosity along with energy and nanoparticles are given. The coupled nonlinear differential equations are solved analytically with the help of the homotopy analysis method (HAM). The convergence of the solution is discussed through h-curves. The physical features of pertinent parameters are discussed by plotting graphs.

Key words: Coaxial Cylinders; Variable Viscosity; Analytical Solution; Non-Newtonian Nanofluid.

1. Introduction

The study of non-Newtonian fluids in the presence of heat transfer analysis has received a great boost and a renewed interest in recent years because of their increasing demand in industry and technology. Some important theoretical studies on this topic are given in [1 – 8].

Recently, a special attention has been given to the nanofluids. The term nanofluid was introduced by Choi 1995 [9] and means a liquid containing a suspension of submicron solid particles (nano particles). The major advantage of nanofluids is their thermal conductivity enhancement (see Masuda et al. [10]). According to Buongiorno and Hu [11], the major use of nanofluids technology is in advance nuclear systems. A comprehensive study about natural convection of nanofluids has been done by Putra et al. [12]. They experimentally discussed the natural convection of nanofluids inside a horizontal cylinder heated from one end and cooled from the other end. Kuznetsov and Nield [13] have examined the natural convective boundary layer flow of a nanofluid past a vertical plate. In another study, Nield and Kuznetsorv [14] have reported the thermal instability in a porous medium layer saturated by a nanofluid. A numerical study about boundary layer flow of a nanofluid past a stretching sheet has been presented by Khan and Pop [15].

The above studies show that there is a strong need to investigate the non-Newtonian nanofluids. Therefore, the aim of the present investigation is to discuss the non-Newtonian nanofluids between two coaxial cylinders. The governing equations of non-Newtonian fluids along with nanoparticles equations have been derived in the presence of variable viscosity. The coupled nonlinear equations have been solved analytically with the help of the homotopy analysis method (HAM) [16 – 22] for two cases of viscosity, namely Reynolds and Vogels viscosity models. The expressions of velocity, temperature, and nanoparticles functions are discussed graphically for different physical parameters.

2. Problem Statement

Consider an incompressible and thermodynamic third-grade nano fluid between two infinite coaxial vertical cylinders. The flow is induced by a constant pressure gradient and motion of an inner cylinder. The outer cylinder is kept fixed. The heat transfer analysis is also taken into account. The dimensionless problems which can describe the flow and heat transfer are

$$\frac{\mathrm{d}\mu}{\mathrm{d}r}\frac{\mathrm{d}v}{\mathrm{d}r}+\frac{\mu}{r}\left(\frac{\mathrm{d}v}{\mathrm{d}r}+r\frac{\mathrm{d}^2v}{\mathrm{d}r^2}\right) + \frac{\Lambda}{r}\left(\frac{\mathrm{d}v}{\mathrm{d}r}\right)^2\left(\frac{\mathrm{d}v}{\mathrm{d}r}+3r\frac{\mathrm{d}^2v}{\mathrm{d}r^2}\right)+G_r\theta+B_r\Phi=C\,, \tag{1}$$

© 2012 Verlag der Zeitschrift für Naturforschung, Tübingen · http://znaturforsch.com

$$r\alpha\frac{\mathrm{d}^2\theta}{\mathrm{d}^2 r}+r\alpha_1\mathrm{Nt}\frac{\mathrm{d}^2\theta}{\mathrm{d}^2 r}+\alpha\frac{\mathrm{d}\theta}{\mathrm{d}r}+r\mathrm{Nb}\frac{\mathrm{d}\Phi}{\mathrm{d}r}\frac{\mathrm{d}\theta}{\mathrm{d}r}=0\,, \quad (2)$$

$$\mathrm{Nb}\left(\frac{\mathrm{d}^2\Phi}{\mathrm{d}^2 r}+\frac{1}{r}\frac{\mathrm{d}\Phi}{\mathrm{d}r}\right)+\mathrm{Nt}\left(\frac{\mathrm{d}^2\theta}{\mathrm{d}^2 r}+\frac{1}{r}\frac{\mathrm{d}\theta}{\mathrm{d}r}\right)=0\,. \quad (3)$$

The corresponding boundary conditions are

$$v(r)=1\,,\ \Phi(r)=1\,,\ \theta(r)=1\,;\ r=1\,, \quad (4)$$

$$v(r)=0\,,\ \Phi(r)=0\,,\ \theta(r)=0\,;\ r=b\,. \quad (5)$$

The nondimensional quantities used in the above equations are defined as

$$\begin{aligned}
&r=\frac{\bar{r}}{R}\,,\ \theta=\frac{(\bar{\theta}-\theta w)}{(\theta m-\theta w)}\,,\\
&\Phi=\frac{(\bar{\Phi}-\Phi w)}{(\Phi m-\Phi w)}\,,\ \Lambda=\frac{2\beta_3 V_0^2}{R^2\mu_0}\,,\\
&C_1=\frac{\partial p_1}{\partial z}\,,\ B_r=\frac{\left(\rho_p-\rho_{fw}\right)\ R^2\,(\Phi m-\Phi w)\,g}{\mu_0 v_0}\,,\\
&C=\frac{C_1R^2}{\mu_0 V_0}\,,\ v=\frac{\bar{v}}{v_0}\,,\\
&\mu=\frac{\bar{\mu}}{\mu_0}\,,\ G_r=\frac{(1-\Phi w)\ \ \rho_{fw}R^2\,(\theta m-\theta w)\,g}{\mu_0 v_0}\,.
\end{aligned} \quad (6)$$

Here μ_0, V_0, Λ, β_3, θm, θw, Φm, and Φw are reference viscosity, reference velocity, dimensionless non-Newtonian parameter, dimensional third-grade parameter, a reference temperature (the bulk mean fluid temperature), wall temperature, reference mass concentration, and wall nanoparticle concentration, respectively.

3. Solution of the Problem

Following Nadeem and Ali [5], the solution is considered for two models of variable viscosity, as follows.

4. Series Solutions for Reynolds' Model

In this case, the viscosity is a function of temperature and is expressed in the form of an exponential function:

$$\mu=\mathrm{e}^{-M\theta} \quad (7)$$

which by Maclaurin's series can be written as

$$\mu=1-M\theta+O(\theta^2)\,. \quad (7a)$$

For $M=0$, the above equation corresponds to the case of constant viscosity. Making use of (7), (1)–(3) take the following form:

$$\begin{aligned}
&\frac{1}{r}\frac{\mathrm{d}v}{\mathrm{d}r}+\frac{\mathrm{d}^2v}{\mathrm{d}r^2}-\frac{M}{r}\theta\frac{\mathrm{d}v}{\mathrm{d}r}-M\theta\frac{\mathrm{d}^2v}{\mathrm{d}r^2}+\frac{\Lambda}{r}\left(\frac{\mathrm{d}v}{\mathrm{d}r}\right)^3\\
&+3\Lambda\frac{\mathrm{d}^2v}{\mathrm{d}r^2}\left(\frac{\mathrm{d}v}{\mathrm{d}r}\right)^2-M\frac{\mathrm{d}\theta}{\mathrm{d}r}\frac{\mathrm{d}v}{\mathrm{d}r}+G_r\theta+B_r\Phi=C\,,
\end{aligned} \quad (8)$$

$$\begin{aligned}
&r\alpha\frac{\mathrm{d}^2\theta}{\mathrm{d}r^2}+r\alpha_1\mathrm{Nt}\frac{\mathrm{d}^2\theta}{\mathrm{d}r^2}+\alpha\frac{\mathrm{d}\theta}{\mathrm{d}r}+r\mathrm{Nb}\frac{\mathrm{d}\Phi}{\mathrm{d}r}\frac{\mathrm{d}\theta}{\mathrm{d}r}\\
&-r\alpha_1M\theta\mathrm{Nt}\frac{\mathrm{d}^2\theta}{\mathrm{d}r^2}+r\theta M\mathrm{Nb}\frac{\mathrm{d}\theta}{\mathrm{d}r}\frac{\mathrm{d}\Phi}{\mathrm{d}r}=0\,,
\end{aligned} \quad (9)$$

$$\begin{aligned}
&\mathrm{Nb}\left(\frac{\mathrm{d}^2\Phi}{\mathrm{d}r^2}+\frac{1}{r}\frac{\mathrm{d}\Phi}{\mathrm{d}r}\right)+\mathrm{Nt}\left(\frac{\mathrm{d}^2\theta}{\mathrm{d}r^2}+\frac{1}{r}\frac{\mathrm{d}\theta}{\mathrm{d}r}\right)\\
&+\mathrm{Nb}M\theta\frac{\mathrm{d}^2\Phi}{\mathrm{d}r^2}+\frac{\mathrm{Nb}M\theta}{r}\frac{\mathrm{d}\Phi}{\mathrm{d}r}-\mathrm{Nt}M\theta\frac{\mathrm{d}^2\theta}{\mathrm{d}r^2}\\
&-\frac{\mathrm{Nt}M\theta}{r}\frac{\mathrm{d}\theta}{\mathrm{d}r}=0\,.
\end{aligned} \quad (10)$$

The solution of above equations have been found analytically by the homotopy analysis method. For HAM solution, we require the following initial guesses:

$$v_0(r)=\frac{(r-b)}{(1-b)}\,, \quad (11)$$

$$\theta_0(r)=\frac{(r-b)}{(1-b)}\,, \quad (12)$$

$$\Phi_0(r)=\frac{(r-b)}{(1-b)}\,. \quad (13)$$

The auxiliary linear operators are

$$\pounds_{vr}(v)=v''\,, \quad (14)$$

$$\pounds_{\theta r}(\theta)=\theta''\,, \quad (15)$$

$$\pounds_{\Phi r}(\theta)=\Phi''\,, \quad (16)$$

which satisfy

$$\mathcal{L}_{vr}(A_1+B_1r)=0\,, \quad (17)$$

$$\mathcal{L}_{\theta r}(A_2+B_2r)=0\,, \quad (18)$$

$$\mathcal{L}_{\Phi r}(A_3+B_3r)=0\,, \quad (19)$$

here $A_1, A_2, B_1, B_2, A_3, B_3$ are the constants.

If $p\in[0,1]$ is an embedding parameter and h_v, h_θ, and h_Φ are the auxiliary parameters, then the problems at the zero and mth-order deformations are defined as

$$\begin{aligned}
&(1-p)\mathcal{L}_v[\,\bar{v}(r,p)-\ v_0(r)]\\
&=p\hbar_vN_v[\,\bar{v}(r,p),\bar{\theta}(r,p),\bar{\Phi}(r,p)]\,,
\end{aligned} \quad (20)$$

$$(1-p)\mathcal{L}_\theta[\,\bar\theta(r,p)-\,\theta_0(r)] = p\hbar_\theta N_\theta[\,\bar v(r,p),\bar\theta(r,p),\bar\Phi(r,p)]\,, \tag{21}$$

$$(1-p)\mathcal{L}_\Phi[\,\bar\Phi(r,p)-\,\Phi_0(r)] = p\hbar_\Phi N_\Phi[\,\bar v(r,p),\bar\theta(r,p),\bar\Phi(r,p)]\,, \tag{22}$$

$$\mathcal{L}_v[v_m(r)-\chi_m v_{m-1}(r)] = \hbar_v R_v(r)\,, \tag{23}$$

$$\mathcal{L}_\theta[\theta_m(r)-\chi_m\theta_{m-1}(r)] = \hbar_\theta R_\theta(r)\,, \tag{24}$$

$$\mathcal{L}_\Phi[\Phi_m(r)-\chi_m\Phi_{m-1}(r)] = \hbar_\Phi R_\Phi(r)\,, \tag{25}$$

$$\bar v(r,p)=\bar\theta(r,p)=\bar\Phi(r,p)=1,\ \ r=1\,, \tag{26}$$

$$\bar v(r,p)=\bar\theta(r,p)=\bar\Phi(r,p)=0,\ \ r=b\,, \tag{27}$$

$$\bar v_m(r,p)=\bar\theta_m(r,p)=\bar\Phi_m(r,p)=0,\ \ r=1\,, \tag{28}$$

$$\bar v_m(r,p)=\bar\theta_m(r,p)=\bar\Phi_m(r,p)=0,\ \ r=b\,. \tag{29}$$

In the above equations, the nonlinear operators for velocity, temperature, and nanoparticles are defined as

$$N_v[\,\bar v(r,p),\bar\theta(r,p),\bar\Phi(r,p)] = \frac{1}{r}\frac{\mathrm{d}v}{\mathrm{d}r}+\frac{\mathrm{d}^2v}{\mathrm{d}r^2} - \frac{M}{r}\theta\frac{\mathrm{d}v}{\mathrm{d}r}-M\theta\frac{\mathrm{d}^2v}{\mathrm{d}r^2}+\frac{\Lambda}{r}\left(\frac{\mathrm{d}v}{\mathrm{d}r}\right)^3 + 3\Lambda\frac{\mathrm{d}^2v}{\mathrm{d}r^2}\left(\frac{\mathrm{d}v}{\mathrm{d}r}\right)^2 - M\frac{\mathrm{d}\theta}{\mathrm{d}r}\frac{\mathrm{d}v}{\mathrm{d}r}+G_r\theta+B_r\Phi-C\,, \tag{30}$$

$$N_\theta[\,\bar v(r,p),\bar\theta(r,p),\bar\Phi(r,p)] = r\alpha\frac{\mathrm{d}^2\theta}{\mathrm{d}r^2} + r\alpha_1\mathrm{Nt}\frac{\mathrm{d}^2\theta}{\mathrm{d}r^2}+\alpha\frac{\mathrm{d}\theta}{\mathrm{d}r}+r\mathrm{Nb}\frac{\mathrm{d}\Phi}{\mathrm{d}r}\frac{\mathrm{d}\theta}{\mathrm{d}r} - r\alpha_1 M\theta\mathrm{Nt}\frac{\mathrm{d}^2\theta}{\mathrm{d}r^2}+r\theta M\mathrm{Nb}\frac{\mathrm{d}\theta}{\mathrm{d}r}\frac{\mathrm{d}\Phi}{\mathrm{d}r}\,, \tag{31}$$

$$N_\Phi[\,\bar v(r,p),\bar\theta(r,p),\bar\Phi(r,p)] = \mathrm{Nb}\left(\frac{\mathrm{d}^2\Phi}{\mathrm{d}r^2}+\frac{1}{r}\frac{\mathrm{d}\Phi}{\mathrm{d}r}\right) + \mathrm{Nt}\left(\frac{\mathrm{d}^2\theta}{\mathrm{d}r^2}+\frac{1}{r}\frac{\mathrm{d}\theta}{\mathrm{d}r}\right)+\mathrm{Nb}M\theta\frac{\mathrm{d}^2\Phi}{\mathrm{d}r^2} + \frac{\mathrm{Nb}M\theta}{r}\frac{\mathrm{d}\Phi}{\mathrm{d}r}-\mathrm{Nt}M\theta\frac{\mathrm{d}^2\theta}{\mathrm{d}r^2}-\frac{\mathrm{Nt}M\theta}{r}\frac{\mathrm{d}\theta}{\mathrm{d}r}\,. \tag{32}$$

$$R_v = -M\sum_{k=0}^{m-1}v'_{m-1-k}\theta'_k+\frac{1}{r}v'_{m-1}-\frac{M}{r}\sum_{k=0}^{m-1}v'_{m-1-k}\theta_k + v''_{m-1}-M\sum_{k=0}^{m-1}v''_{m-1}\theta_k+\frac{\Lambda}{r}\sum_{k=0}^{m-1}\sum_{l=0}^{k}v'_{m-1-k}v'_{k-l}v'_l + 3\Lambda\sum_{k=0}^{m-1}\sum_{l=0}^{k}v'_{m-1-k}v'_{k-l}v''_l+G_r\theta_{m-1} + B_r\Phi_{m-1}-C(1-\chi_m)\,, \tag{33}$$

$$R_\theta = \frac{\alpha}{r}\theta'_{m-1}+\theta''_{m-1}+\alpha_1\mathrm{Nt}\theta''_{m-1} + \alpha_1\mathrm{Nt}M\sum_{k=0}^{m-1}\theta''_{m-1-k}\theta_k+\mathrm{Nb}\sum_{k=0}^{m-1}\Phi_{m-1-k}\theta'_k + M\mathrm{Nb}\sum_{k=0}^{m-1}\Phi'_{m-1-k}\sum_{l=0}^{k}\theta'_{k-l}\theta_l\,, \tag{34}$$

$$R_\Phi = \frac{\mathrm{Nb}}{r}\Phi'_{m-1}+\mathrm{Nb}\Phi''_{m-1}+\mathrm{Nb}M\sum_{k=0}^{m-1}\Phi''_{m-1-k}\theta_k + \frac{\mathrm{Nb}M}{r}\sum_{k=0}^{m-1}\Phi'_{m-1-k}\theta_k+\mathrm{Nt}\theta''_{m-1}+\frac{\mathrm{Nt}}{r}\theta'_{m-1} - \mathrm{Nt}M\sum_{k=0}^{m-1}\theta''_{m-1-k}\theta_k-\frac{\mathrm{Nt}M}{r}\sum_{k=0}^{m-1}\theta'_{m-1-k}\theta_k\,. \tag{35}$$

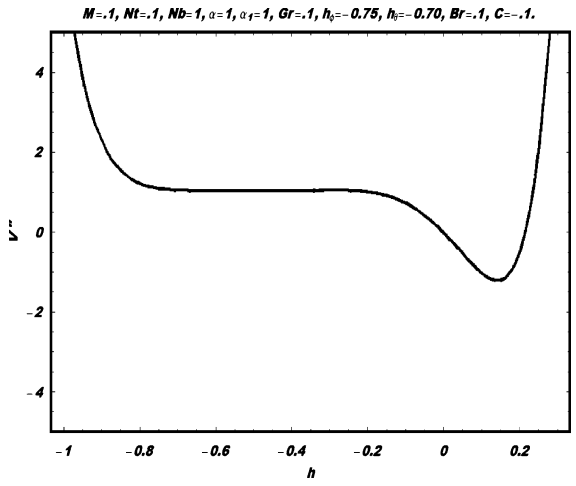

Fig. 1. h-curve for the velocity profile for the Reynolds model.

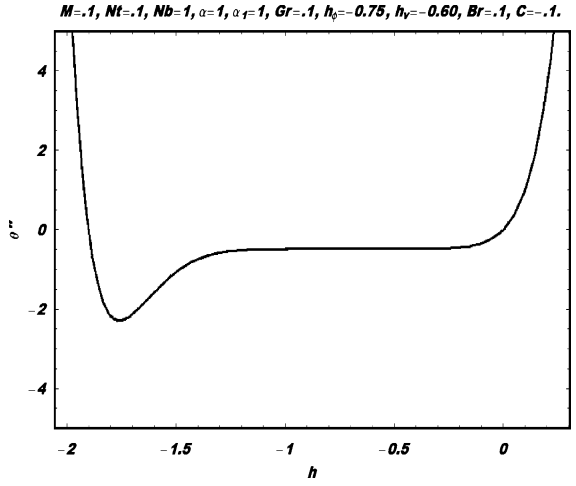

Fig. 2. h-curve for the temperature profile for the Reynolds model.

By Mathematica, the solutions can be written as

$$v = \sum v_m(r) = \sum_{n=0}^{3m+1} a_{m,n} r^n, \quad m \geq 0,$$
$$\theta = \sum \theta_m(r) = \sum_{n=0}^{3m+1} d_{m,n} r^n, \tag{36}$$
$$\Phi = \sum \Phi_m(r) = \sum_{n=0}^{3m} e_{m,n} r^n, \quad m \geq 0,$$

where $a_{m,n}$, $d_{m,n}$, and $e_{m,n}$ are constants to be determined by substituting (36) into (20)–(22).

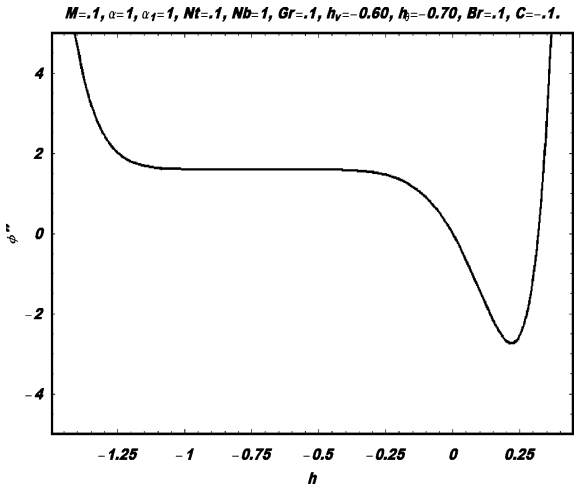

Fig. 3. h-curve for the nanoparticle concentration profile for the Reynolds model.

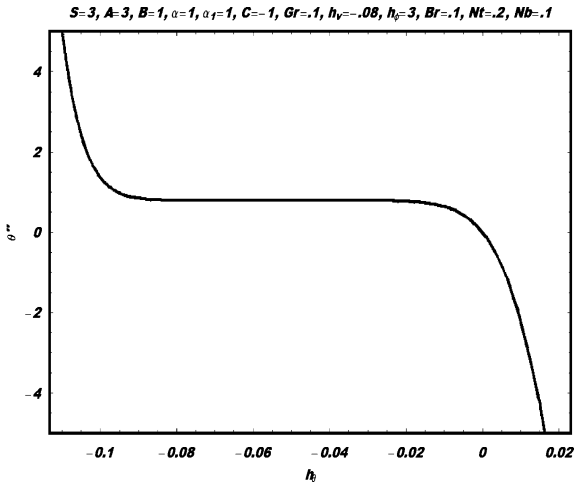

Fig. 5. h-curve for the temperature profile for the Vogel model.

5. Series Solutions for Vogel's Model

Here, the viscosity is defined as

$$\mu = \mu_0 \exp\left[\frac{A}{(B+\theta)} - \theta_0\right], \tag{37}$$

which can also be written as

$$\mu = \frac{C}{s}\left(1 - \frac{\theta A}{B^2}\right), \tag{38}$$

where

$$s = \mu_0 \exp\left[\frac{A}{B} - \theta_0\right]. \tag{39}$$

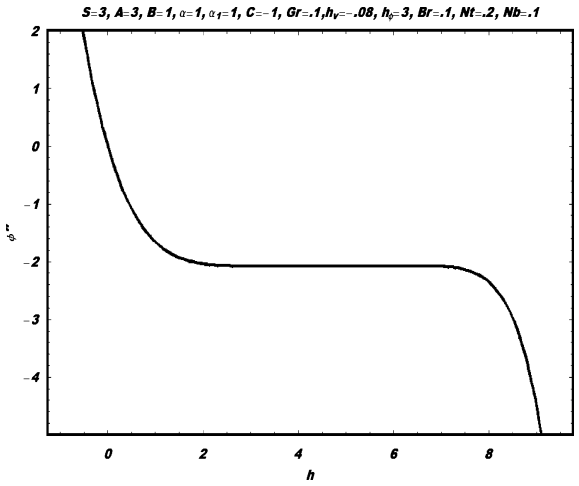

Fig. 4. h-curve for the nanoparticle concentration profile for the Vogel model.

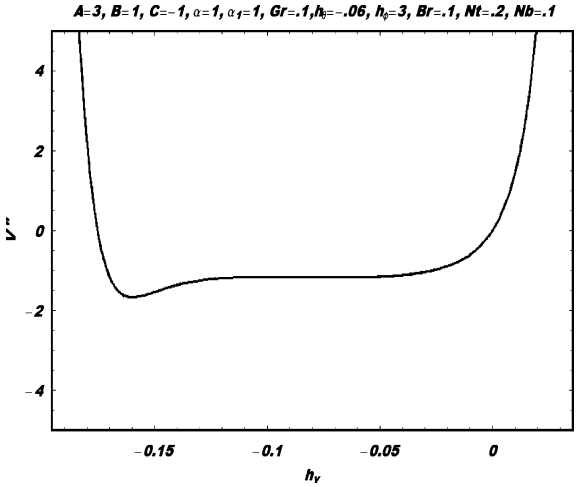

Fig. 6. h-curve for the velocity profile for the Vogel model.

Using the similar procedure as discussed in previous section, the solution of this case is straightforward written as

$$v = \sum v_m(r) = \sum_{n=0}^{3m+1} a'_{m,n} r^n, \quad m \geq 0,$$
$$\theta = \sum \theta_m(r) = \sum_{n=0}^{3m+1} d'_{m,n} r^n, \tag{40}$$
$$\Phi = \sum \Phi_m(r) = \sum_{n=0}^{3m} e'_{m,n} r^n, \quad m \geq 0,$$

where $a'_{m,n}$, $d'_{m,n}$, and $e'_{m,n}$ are constants.

6. Graphical Results and Discussion

The convergence of the obtained series solutions and the effects of pertinent parameters in the present investigation are reported through Figures 1 – 15. The variations of Nt, Nb, A, and B are observed. Figures 1 – 3 have been plotted for Reynolds' model. Figure 1 is prepared to see the convergence region for the velocity profile. Figure 2 is prepared to see the convergence region for the temperature profile. Figure 3 is prepared to see the convergence region for the nanoparticle concentration profile. Figures 4 – 6 are prepared to see the convergence region for the nanopar-

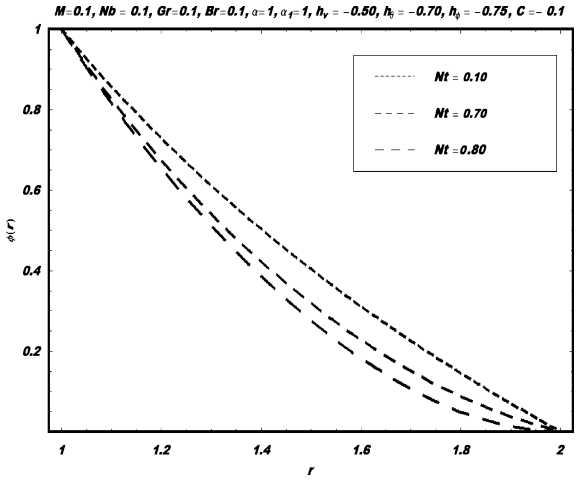

Fig. 7. Nanoparticle concentration profile along radial distance for different values of Nt for the Reynolds model.

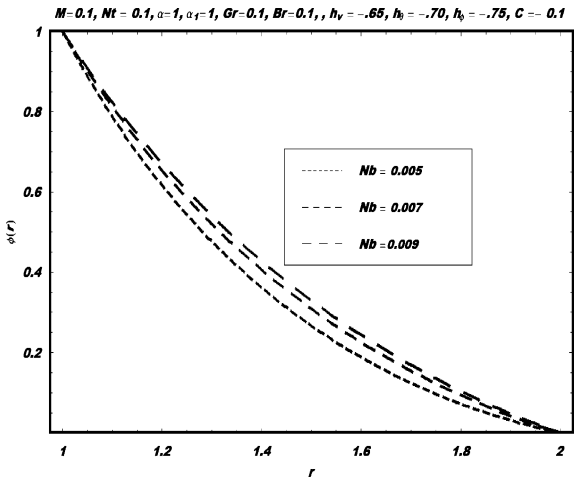

Fig. 8. Nanoparticle concentration profile along radial distance for different values of Nb for the Reynolds model.

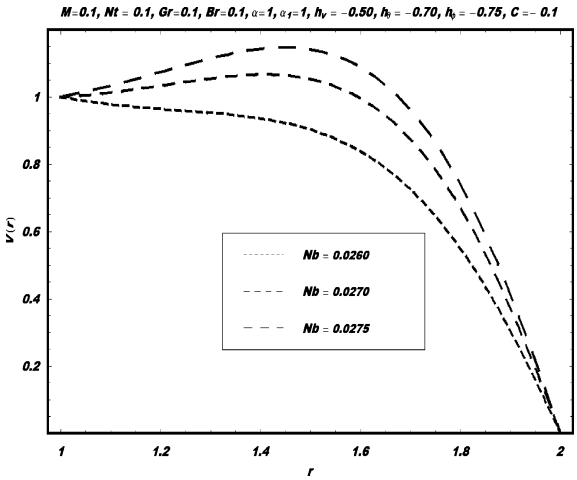

Fig. 9. Velocity profile along radial distance for different values of Nb for the Reynolds model.

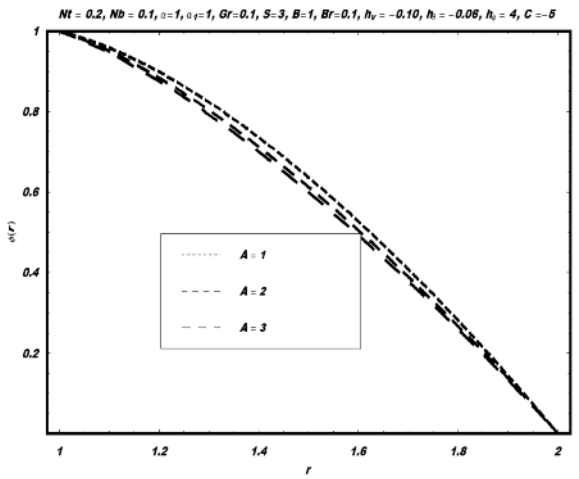

Fig. 10. Temperature profile along radial distance for different values of A for the Vogel model.

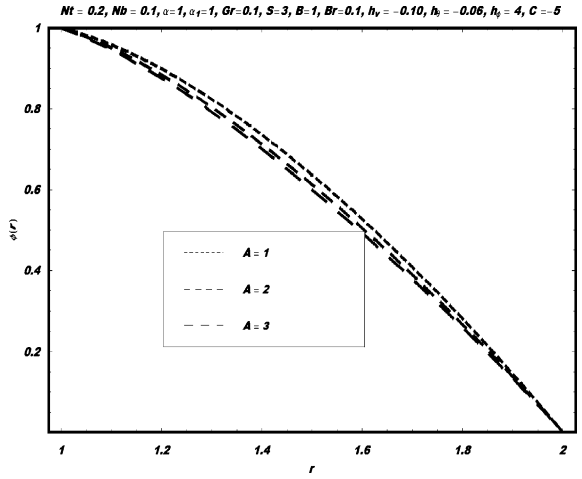

Fig. 11. Nanoparticle concentration profile along radial distance for different values of A for the Vogel model.

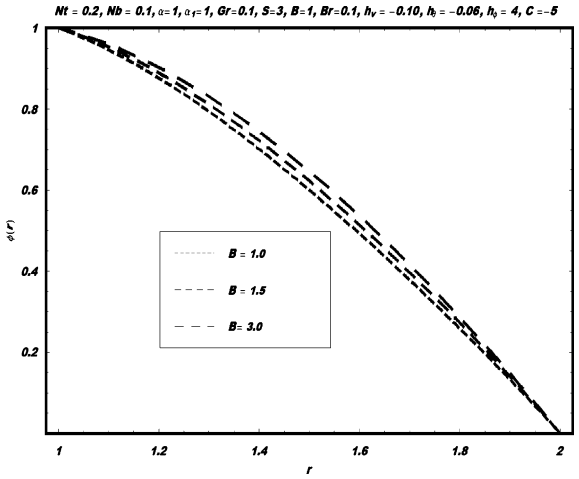

Fig. 12. Nanoparticle concentration profile along radial distance for different values of B for the Vogel model.

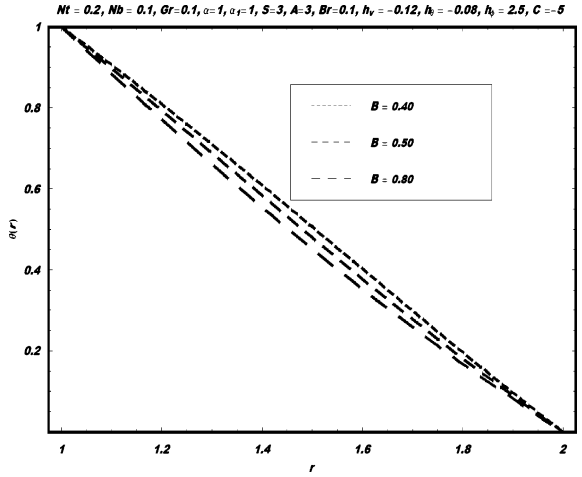

Fig. 13. Temperature profile along radial distance for different values of B for the Vogel model.

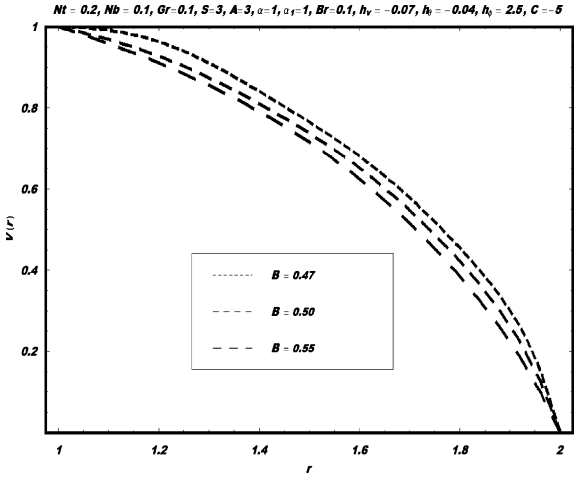

Fig. 14. Velocity profile along the radial distance for different values of B for the Vogel model.

ticle concentration, temperature, and velocity profiles for the Vogel model. Figures 7 – 9 have been plotted for Reynolds' model. Figure 7 is prepared for the nanoparticle concentration distribution when different values of Nt are used. It can be seen that with an increase in Nt the nanoparticle concentration profile decreases. Figure 8 is plotted for the nanoparticle concentration when different values of Nb are used. It is observed that with an increase in Nb the nanoparticle concentration profile increases. Figure 9 is prepared in order to observe the behaviour of velocity profiles for different values of Nb. It is observed that the velocity profile increases with an increase in Nb. Figures 10 – 15 have been plotted for Vogel's model. Figures 10 – 11 are plotted for the nanoparticle concentration and temperature profiles for different values of A. It is observed that the temperature increases and the nanoparticles concentration profiles decreases with rise in A. The nanoparticle concentration, temperature, and velocity profiles are seen in Figures 12 – 14 for different values of the viscosity parameter B. Figure 15 is plotted for the nanoparticles concentration for different values of

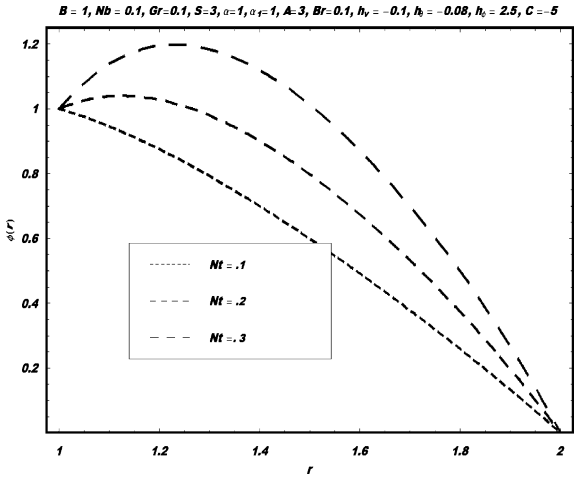

Fig. 15. Nanoparticle concentration profile along radial distance for different values of Nt for the Vogel model.

Nt. It can be seen that this profiles increases with an increase in Nt.

Table 1. Convergence table for the Reynolds model for $M = 0.1$, $\Lambda = 0.001$, $G_r = 0.1$, $\alpha = 1$, $\alpha_1 = 1$, $B_r = 0.1$, $h_\theta = -0.70$, $h_\phi = -0.75$, $h_v = -0.65$, $Nt = 0.1$, and $C = -0.1$.

Order of approximation	$\lvert v''(1)\rvert$	$\lvert\theta''(1)\rvert$	$\lvert\phi''(1)\rvert$
5	1.52960	1.42838	0.005
10	1.53939	1.44088	0.006
15	1.53917	1.44093	0.006
20	1.53917	1.44093	0.006
25	1.53917	1.44093	0.006
30	1.53917	1.44093	0.006
35	1.53917	1.44093	0.006

Acknowledgement

We would like to thank the anonymous referees for their very expertise comments for the improvement of the paper. First author also wishes to thank the Quaid-i-Azam University, Islamabad, on providing financial support.

[1] M. Massoudi and I. Christie, Int. J. Nonlin. Mech. **30**, 687 (1995).
[2] T. Hayat, R. Ellahi, and S. Asghar, Commun. Nonlin. Sci. **12**, 300 (2007).
[3] M. Yurusoy and M. Pakdermirli, Int. J. Nonlin. Mech. **37**, 187 (2002).
[4] M. Pakdermirli and B. S. Yilbas, Int. J. Nonlin. Mech. **41**, 432 (2006).
[5] S. Nadeem and M. Ali, Commun. Nonlin. Sci. **14**, 2070 (2009).
[6] S. Nadeem, T. Hayat, S. Abbasbandy, and M. Ali, Nonlin. Anal: Real World Appl. **11**, 856 (2010).
[7] R. Ellahi and S. Afzal, Commun. Nonlin. Sci. **14**, 2056 (2009).
[8] M. Y. Malik, A. Hussain, S. Nadeem, and T. Hayat, Z. Naturforsch. **64a**, 588 (2009).
[9] S. Choi, Enhancing thermal conductivity of fluids with nanoparticle in: D. A. Siginer, H. P. Wang (Eds.), Developments and Applications of Non-Newtonian flows, ASME MD Vol. 231 and PED Vol. 66. 1995, pp. 99 – 105.
[10] H. Masuda, A. Ebata, K. Teramae, and M. Hishinuma, Netsu Bussei **7**, 227 (1993).
[11] J. Buongiorno and W. Hu, Nanofluid coolants for advanced nuclear power plants, Paper no. 5705, Proceedings of ICAPP '05. Seoul, May 15 – 19, 2005.
[12] N. Putra, W. Roetzel, and S. K. Das, Heat Mass Transfer **39**, 775 (2003).
[13] A. V. Kuznetsov, D. A. Nield, Int. J. Therm. Sci. **49**, 243 (2010).
[14] D. A. Nield and A. V. Kuznetsov, Int. J. Heat Mass Tran. **52**, 5792 (2009).
[15] W. A. Khan and I. Pop, Int. J. Heat Mass Transfer **53**, 2477 (2010).
[16] S. J. Liao, Beyond Perturbation: Introduction to Homotopy Analysis Method, Chapman & Hall/CRC Press, Boca Raton 2003.
[17] S. J. Liao, Appl. Math. Comput. **147**, 499 (2004).
[18] S. J. Liao, Fluid Mech. **385**, 101 (1999).
[19] S. J. Liao, Commun. Nonlin. Sci. **11**, 326 (2006).
[20] S. Abbasbandy, Phys. Lett. A **360**, 109 (2006).
[21] S. Abbasbandy, Int. Commun. Heat Mass **34**, 380 (2007).
[22] S. Abbasbandy, Y. Tan, and S. J. Liao, Appl. Math. Comput. **188**, 1794 (2007).